mRNA interactome capture in mammalian cells

Kastelic, N., Landthaler, M.

This is the final version of the accepted manuscript. The original article has been published in final edited form in:

Methods
2017 AUG 15 ; 126: 38-43
2017 JUL 11 (first published online: final publication)
doi: 10.1016/j.ymeth.2017.07.006

Publisher: Elsevier

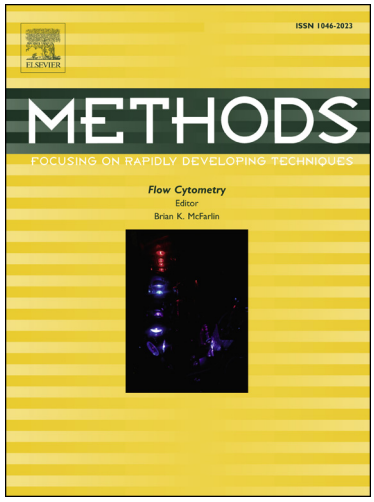

mRNA interactome capture in mammalian cells

Nicolai Kastelic, Markus Landthaler

PII: S1046-2023(16)30408-X
DOI: http://dx.doi.org/10.1016/j.ymeth.2017.07.006
Reference: YMETH 4272

To appear in: *Methods*

Received Date: 9 April 2017
Revised Date: 22 May 2017
Accepted Date: 8 July 2017

Please cite this article as: N. Kastelic, M. Landthaler, mRNA interactome capture in mammalian cells, *Methods* (2017), doi: http://dx.doi.org/10.1016/j.ymeth.2017.07.006

mRNA interactome capture in mammalian cells

Nicolai Kastelic[1] and Markus Landthaler[1,2,*]

[1] RNA Biology and Posttranscriptional Regulation, Max Delbrück Center for Molecular Medicine Berlin, Berlin Institute for Molecular Systems Biology, 13125 Berlin, Germany

[2] IRI Life Sciences, Institut für Biologie, Humboldt-Universität zu Berlin, 10115 Berlin, Germany

*** Correspondence to:**

Markus Landthaler

Max Delbrück Center for Molecular Medicine Berlin

Robert-Roessle Str. 10

13125 Berlin, Germany

email: markus.landthaler@mdc-berlin.de

phone: +49 30 9406 3026

fax: +49 30 9406 49160

Keywords

RNA; RNA-binding protein; RNA-protein interaction; mRNA interactome capture, crosslinking; mass spectrometry

Abstract

Throughout their entire life cycle, mRNAs are associated with RNA-binding proteins (RBPs), forming ribonucleoprotein (RNP) complexes with highly dynamic compositions. Their interplay is one key to control gene regulatory mechanisms from mRNA synthesis to decay. To assay the global scope of RNA-protein interactions, we and others have published a method combining crosslinking with highly stringent oligo(dT) affinity purification to enrich proteins associated with polyadenylated RNA (poly(A)+ RNA). Identification of the poly(A)+ RNA-bound proteome (also: mRNA interactome capture) has by now been applied to a diversity of cell lines and model organisms, uncovering comprehensive repertoires of RBPs and hundreds of novel RBP candidates. In addition to determining the RBP catalog in a given biological system, mRNA interactome capture allows the examination of changes in protein-mRNA interactions in response to internal and external stimuli, altered cellular programs and disease.

1. Introduction

Almost all classes of RNAs are subject to intricate post-transcriptional regulatory control coordinating their maturation, transport, stability and degradation [1]. RNA-binding proteins (RBPs) engage with RNAs to form higher-order ribonucleoprotein (RNP) complexes and act synergistically in order to shape RNA fate [2-5]. The dynamic compositions of RNP complexes provide not only specificity to regulatory processes, but also make post-transcriptional regulation highly responsive to external cues by remodeling of RNP complexes. Thus, regulatory modes are dependent on the abundance of RBPs and the competition between RBPs with overlapping target specificity which facilitates interrogation of posttranscriptional networks by profiling RBPs globally. We and others published the first comprehensive mRNA-binding protein repertoires in mammalian cells by applying a method termed mRNA interactome capture [6, 7]. By now, this approach has been successfully applied to cell lines such as HEK293 [6], HeLa [7], Huh-7 [8], mESC [9], RAW 264.7 [10], HL-1 [11] as well as a diverse set of organisms including *Saccharomyces cerevisiae* [8, 12], *Caenorhabditis elegans* [12], *Drosophila melanogaster* [13, 14], *Arabidopsis thaliana* [15, 16], *Plasmodium falciparum* [17], *Leishmania donovani* [18] and *Danio rerio* [19] .

mRNA interactome capture can be characterized by two features: The formation of covalent bonds between RNAs and proteins induced *in vivo* by UV crosslinking as well as the highly stable bead-coupled oligo(dT)-poly(A) tail hybridization and affinity purification for mRNA enrichment. The combination of both elements allows for stringent purification of poly(A)$^+$ RNA associated protein factors by using elevated amounts of chaotropic agents to eliminate unspecific interactions in otherwise highly complex mixtures (such as concentrated cell extracts).

Similar to crosslinking and immunoprecipitation (CLIP) methods [20-23], covalent bond formation between proteins and RNA is achieved by UV crosslinking, a photo-crosslinking approach for which monochromatic UV light irradiation is used. It induces short-lived free radicals at nucleotide bases resulting in covalent bond formation with amino acids of proteins in direct vicinity (~2 Å, “zero distance”) [24, 25]. Two approaches are commonly used fur UV crosslinking: Conventional UV crosslinking (cCL) uses UV irradiation at 254 nm wavelength to induce covalent bond formation between nucleic acids and proteins. Alternatively, incorporation of photoactivatable ribonucleosides (PARs) such

as 4-thiouridine (4SU) and 6-thioguanosine (6SG) into newly synthesized RNAs to enhance crosslinking (PAR-CL) can be utilized [26]. In this case, UV irradiation at lower-energy 365 nm wavelength initiates covalent bond formations between RNAs and proteins at sites of 4SU and 6SG incorporation.

Despite being the crosslinking approach of choice in combination with mRNA interactome capture, UV irradiation might not always be a feasible choice as light penetration (cCL and PAR-CL) or nucleoside incorporation (PAR-CL) can limit the efficacy of the procedure. For instance, applying UV crosslinking to non-etiolated plants could further reduce efficacy of the approach due to the presence of UV light-absorbing chloroplasts. For organisms that are not transluscent, UV crosslinking could only be successfully applied with extended crosslinking periods [8, 27]. To overcome this limitation, chemical crosslinking using formaldehyde (FA) could be used to covalently crosslink RNA and interacting proteins in a similar fashion as in the RIPiT-seq protocol [28]. Of note, FA crosslinking also induces covalent bond formation between proteins, a feature which can be exploited to stabilize higher-order RNPs.

Here, we provide a protocol suitable for usage with mammalian cell culture systems and show that modifications to the protocol, e.g. the crosslinking approach, can be made. Moreover, we discuss the advantages and shortcomings of the hallmarks of this protocol – crosslinking and oligo(dT) affinity purification – in more detail.

2. Method

2.1. mRNA interactome capture in mammalian cells

As a quick reference guide, we included a step-by-step protocol and troubleshooting section in the Supplemental material which can be used for the bench work.

2.1.1. Cell Culture and crosslinking

Cells are grown in appropriate growth medium and expanded to tissue culture plates with a diameter of 150 mm. Dependent on the cellular system of choice, ~10^7-10^8 cells per sample will be subjected to one out of three crosslinking procedures (a-c). (a) For conventional UV crosslinking (cCL), the culture medium is removed and plates are directly transferred onto ice. Cells are crosslinked with 254 nm UV light (0.15 J/cm^2) on ice using a Stratalinker 2400 (Stratagene). (b) For photoactivatable-ribonucleoside-enhanced

crosslinking (PAR-CL), the cell culture growth medium of cells at 70-80% confluency is supplemented with 4SU for not more than 8 hours of metabolic labeling. We suggest starting with a final concentration of 100 µM or 200 µM 4sU which usually yields good incorporation results while maintaining effects of cellular stress at a minimum [37]. For short labeling times (1-2 hours) higher 4SU concentrations of 600 - 800 mM final concentration can be used. As 4SU incorporation rates into nascent RNA can greatly vary between cellular systems, it is recommended to test labeling efficiencies beforehand. Usually, we use comparison to 4SU incorporation rates observed in HEK293 cells by thiol-specific biotinylation [29] or LC-MS analysis [30]. Of note, global characterization of the RBP repertoire in HEK293 cells can be achieved with 4SU incorporation efficiencies between 1% and 4% [6, 26]. After metabolic labeling, the cell culture growth medium is removed and plates are transferred onto ice. Cells are crosslinked with 365 nm UV light (0.15-0.2 J/cm^2) on ice using a Stratalinker 2400 (Stratagene). (c) For formaldehyde (FA) crosslinking, culture medium is removed and 10 ml of 0.05% to 0.1% formaldehyde solution (in PBS) per plate are added. At room temperature, the plates are gently rocked for 10 minutes and crosslinking is quenched by the addition of 2 ml 1.5M glycine per plate. The plates are rocked for another 5 minutes, aspirated and transferred onto ice. Importantly, we want to point out that the FA crosslinking procedure should be optimized individually for any given cellular system beforehand using the detection of known RBPs by Western analysis as a benchmark (see 2.2.3.). In particular, elevated FA concentrations and excessive incubation times favor accumulation of crosslinking of non-native interaction events which should be minimized. (a-c) 3 ml of ice-cold PBS per plate are added, cells are scraped off with a rubber policeman and collected in a pre-cooled falcon by centrifugation. Cell pellets are washed at least once in ice-cold PBS followed by centrifugation and flash-freezing in liquid nitrogen for long-term storage (alternatively, proceed to section 2.1.2 immediately).

2.1.2. Preparation of cell lysate and oligo(dT) pulldown

Cell pellets are lysed in 10 pellet volumes of lysis/binding buffer (100 mM Tris-HCl, pH 7.5 at 25°C, 500 mM LiCl, 10 mM EDTA, pH 8.0 at 25°C, 1% LiDS, add freshly: 5 mM DTT, Mini EDTA-free protease inhibitor (Roche)) by gentle pipetting until being fully resuspended. Following an incubation time of 15 minutes at room temperature, further homogenization and genomic DNA shearing are achieved by passing the lysate 10 times through a 21 gauge needle and once through a 26 gauge needle. At times, lysates may turn out to be viscous, pointing towards a suboptimal ratio of cell material to lysis/binding buffer. In order to not affect the oligo(dT) pulldown, it is recommended to adjust the amount of

lysis/binding buffer accordingly. The Dynabeads mRNA DIRECT oligo(dT) beads (Thermo Fisher Scientific) are washed once in one original suspension volume of lysis/binding buffer. Typically, an equivalent of 2 ml Dynabead suspension (bed volume: ~15 µl), as provided by the manufacturer, is used for a lysate of 10^8 cells. After adding the oligo(dT) beads, lysates are incubated for 1 hour at room temperature on a rotating wheel. While RNA is usually processed at low temperatures in order to preserve its integrity, we do not recommend lowering the incubation temperature to avoid precipitation of LiDS which may impede binding of the oligo(dT) beads to RNA. Subsequently, the oligo(dT) beads are concentrated on a magnetic rack, lysates are transferred into new tubes and stored on ice for multiple rounds of oligo(dT) pulldown. Beads are washed three times in one lysate volume of lysis/binding buffer containing 1% of lithium dodecyl sulfate (LiDS). While the LiDS concentration in the lysis/binding buffer may be decreased in order to improve overall yield of the affinity purification, it is not recommended, as it would be at the expense of stringency and likely specificity of the poly(A)$^+$ RNA-bound protein enrichment. Further three rounds of washes are performed in one lysate volume of NP40 Washing buffer (50 mM Tris-HCl, pH 7.5 at 25°C, 140 mM LiCl, 2 mM EDTA, pH 8.0 at 25°C, 0.5% NP-40, add freshly: 0.5 mM DTT, Mini EDTA-free protease inhibitor (Roche)) followed by heat elution (80°C, 2 min) of crosslinked poly(A)$^+$ RNA-protein complexes in 300 µl low-salt elution buffer. Before resuspending the oligo(dT) beads in the low-salt elution buffer, it is highly recommended to ensure full removal of leftover NP40 Washing buffer. Carryover of detergents may cause issues for downstream mass spectrometry applications. Implementation of one additional round of washing in one lysate volume of detergent-free washing buffer (50 mM Tris-HCl, pH 7.5 at 25°C, 140 mM LiCl, 2 mM EDTA, pH 8.0 at 25°C, add freshly: 0.5 mM DTT, Mini EDTA-free protease inhibitor (Roche)) may solve detergent-related problems. While the eluate is stored on ice, the oligo(dT) beads are re-incubated with the lysate for a total of three rounds of oligo(dT) hybridization by repeating the described procedure. Eluates are combined and stored at -80°C (alternatively, proceed to section 2.1.3).

2.2. Downstream applications

Eluates from the oligo(dT) enrichment protocol described in section 2.1 consist of crosslinked proteins (RBPs), crosslinked poly(A)$^+$ RNA and non-crosslinked poly(A)$^+$ RNA.

2.2.1. RNase treatment

Following oligo(dT) affinity purification of crosslinked poly(A)$^+$ RNA-protein complexes, proteins are released by RNA digestion in order to allow for further analysis. Incubating the eluate with RNase I (and optionally: Benzonase) at a final concentration of 0.1 U/µl in the presence of 1mM $MgCl_2$ for a minimum of one hour at 37 °C is sufficient to fully recover the proteins. At this point, proteins can be directly subjected to mass spectrometry sample preparation.

2.2.2. Protein quality control: SDS-PAGE

To control for efficient enrichment of poly(A)$^+$ RNA-bound proteins in the oligo(dT) eluate, 5% of the total eluate are used for analysis by SDS-PAGE. Figure 2 shows a representative silver stained SDS-PAGE gel for all three discussed crosslinking approaches. For all crosslinked and oligo(dT) affinity purified samples, characteristic patterns of protein bands distinct from the input control are visible. More so, our stringent oligo(dT) affinity purification protocol described here clearly supports enrichment of specific poly(A)$^+$ RNA by oligo(dT) hybridization over unspecific interactions as in the non-crosslinked controls. We would like to note that in order to reduce background of the oligo(dT) pulldown to a minimum, proper resuspension of the beads during each round of washing is mandatory. Further reduction of background may be achieved by prolonged washing phases (one to three minutes on a rotating wheel at room temperature). Another factor subject to optimization is the amount of oligo(dT) beads used per sample. Preliminary calculations on total RNA yield per sample and small scale oligo(dT) pulldowns may indicate if the amount of beads used should be maintained or decreased according to the oligo(dT) beads binding capacity (as provided by the manufacturer). We strongly suggest to not deliberately use an excess of beads as this may increase the amount of co-purifying contaminants, and therefore background. The number of oligo(dT) affinity purification rounds should not be altered. In our previous work, we found that while multiple rounds of oligo(dT) pulldown may be beneficial to capture lowly abundant transcripts as well as transcripts with shorter poly(A) tails, further rounds of hybridization increase the amount of co-purifying contaminating RNA species such as ribosomal RNAs. With three rounds of oligo(dT) affinity purification, we were able to deplete 80% to 90% of mRNAs in cell lysates [6].

2.2.3. Protein quality control: Western analysis

While running a SDS-PAGE sheds light onto how technical aspects of the mRNA interactome protocol worked, it does not reveal if the enrichment is specific for RBPs. A straightforward way to explore mRNA

interactome samples for specific enrichment of RBPs is to run a Western Blot. In the interest of monitoring RBP enrichment and non-RBP depletion, we suggest to save a small fraction of the input lysate (0.1% is sufficient) when performing the mRNA interactome protocol to assay with the eluate. Alongside your protein(s) of interest, we recommend adding a positive control (e.g. any of the hnRNP proteins – should be enriched in the eluate) and a negative control (e.g. tubulin – should be depleted in the eluate).

2.2.4. poly(A)$^+$ depletion control

To measure the degree of poly(A)$^+$ RNA depletion when applying the mRNA interactome protocol, quantitative Real-Time PCR (qRT-PCR) can be performed. The mRNA content after each round of oligo(dT) affinity purification as compared to the input can be estimated by assaying highly abundant transcripts of genes like GAPDH, TUBB or ACTA1/ACTB (positive control, polyadenylated) and compared to 18s rRNA (negative control, not polyadenylated) [6].

2.2.5. Mass Spectrometry

Proteome-wide detection of enriched RBPs can be achieved with mass spectrometry. Therefore, eluates from the mRNA interactome capture protocol need to be further processed. In short, eluates are subjected to TCA precipitation and resuspended in 8M Urea solution to concentrate and denature proteins. Disulfide bonds are reduced by adding dithiothreitol (DTT), followed by alkylation of sulfhydryl groups from cysteins with iodoacetamide (IAA) to irreversibly prevent reformation of disulfide bonds. Proteins are separated by SDS-PAGE and proteins are in-gel digested with Lys-C and trypsin. Resulting peptides are further concentrated and desalted with C18 column purification, strong cation exchange chromatography columns (SCX) and a second round of C18 column purification. The final peptide mixture can be measured with Liquid Chromatography-Tandem Mass Spectrometry (LC-MS/MS). Identification of proteins/peptides can be performed using MaxQuant [38].

2.3. Identification of RBPs in mRNA interactome capture mass spectrometry data

We commonly use the label-free quantification (LFQ) approach as a relative quantification method for proteins across replicates and samples [39]. To apply statistical analysis, mean log fold-changes of

proteins identified in crosslinked samples over non-crosslinked control across replicates are generated using intensities. At this point, proteins with fold-changes that equal 0 (not enriched in crosslinked sample over non-crosslinked control) or smaller 0 (enriched in the non-crosslinked control over the crosslinked sample) are likely to be unspecifically co-purified during the mRNA interactome capture protocol. Next, significance for differential enrichment can be inferred using a t-test or empirical Bayes moderated t-test. Calculated p-values are not sufficient for proper interpretation of mRNA interactome capture data: As we are handling high dimensional data involving proteins with different abundance levels, RNA-binding modes and crosslinking probabilities which can influence identification and quantification of recovered proteins, multiple testing has to be performed to estimate the false discovery rate (FDR). By applying the Benjamini and Hochberg method and choosing a cutoff for the FDR (e.g. < 0.01), p-values will be adjusted accordingly (hence: p adj). Proteins which are not enriched or enriched with a FDR above 0.01 can be discarded from further analysis and are not identified as RBPs in this experimental setup. All other proteins which are enriched with a FDR below 0.01 are identified as RBPs by mRNA interactome capture, but by setting the FDR threshold to 0.01, we accept that 1% of those proteins are false positives.

3. Discussion

3.1. RNA-protein crosslinking

UV crosslinking is the approach of choice for stabilization of RNA-protein interactions by covalent bond formation in our mRNA interactome protocol. Still, application of UV irradiation has its shortcomings. As shortly mentioned before, it is not applicable across biological systems with the same crosslinking efficacy. In general, the occurrence of crosslinking events is inherently low and taken together, both factors may impair successful stabilization of RNA-protein interactions. Another aspect that should be taken into consideration is that UV crosslinking is not unbiased. For cCL, potentially all four ribonucleosides can form photoadducts, but pyrimidines are more efficient crosslinking bases than purines [24]. In regards of PAR-CL, short labeling pulses with 4SU or 6SG can be utilized to increase crosslinking efficiency for certain RBPs [7]. On the other hand, RNA-protein interactions on uridine- or guanosine-poor transcripts might be underrepresented and not fully retrieved. Even for RBPs that can be readily UV crosslinked, differences between the cCL and the PAR-CL approaches can be observed that arise from the transcript sequence itself [7]. FA crosslinking might avoid these nucleotide composition-dependent pitfalls. The underlying chemical crosslinking reaction consists of two consecutive

nucleophilic additions which crosslinks any biomolecule with another if both contain nucleophilic moieties and are proximal. In contrast to UV crosslinking which retrieves direct RNA-protein interactions exclusively, FA induced crosslinking enables stabilization of indirect RNA-binding factors as constituents of higher-order RNPs [28]. Here, we only provide a proof-of-principle showing that FA crosslinking can be combined with the mRNA interactome capture affinity purification protocol (Fig. 2). The crosslinking procedure itself should be further optimized to avoid false positive crosslinking events in order to maximize the yield of true interactions.

3.2. oligo(dT) affinity purification

mRNA interactome capture is a protocol to enrich mRNAs and their crosslinked adducts on a global scale. It exploits the presence of 3' polyadenylation which is a common feature of mRNAs. mRNA should be captured from the moment the poly(A) tail is added until the removeal of the tail and mRNA decay. Since introns can be spliced posttranscriptionally or are tained [40], RBPs bound to these introns are likely identified by mRNA interactome capture. Unlike most mRNAs, histone mRNAs are not polyadenylated [33] and therefore not captured with our protocol. For polyadenylated mRNAs, the length of their poly(A) tails can vary greatly [33-35]. While there is still ongoing debate about the true range of poly(A) tail lengths [33], we do not expect the length of poly(A) tails to influence enrichment with our mRNA interactome capture protocol for most parts. It is a possibility that poly(A) tails shorter than 20 nucleotides might not be as efficiently captured as transcripts with longer poly(A) tails as the poly(A)-oligo(dT) hybridization becomes increasingly less stable.

Besides, mRNA interactome capture does not only enrich mRNAs. lncRNAs are transcribed in a RNA polymerase II-dependent manner and many are polyadenylated [36], which impedes biochemical discrimination between mRNAs and lncRNA in our protocol. Therefore, a small subset of interacting proteins captured in our protocol can most likely be contributed to protein-lncRNA interaction.

4. Concluding remarks

Here, we provide a detailed protocol for mRNA interactome capture to enrich RBPs bound and crosslinked to poly(A)$^+$ RNA. While single aspects of this protocol may be altered according to the experimenters needs and the biological system of interest, the overall framework is robust and highly

reproducible. One central future task is to expand the applicability of the approach to non-polyadenylated RNAs to provide a more complete snapshot of the RBP repertoire. More importantly, RNA interactome capture could be applied for comparative studies. Different RBPs within a single biological sample should not be compared as crosslinking biases will lead to misleading interpretations. In contrast, quantifying the enrichment of individual RBPs across different biological samples will give valuable insights into how the interactions of proteins with RNA are altered on a global scale, providing cues as to how dynamic protein-mRNA interactions are leading to plastic post-transcriptional regulatory mechanisms.

5. References

[1] M.J. Moore, Science 309 (2005) 1514.

[2] J.D. Keene, Nat. Rev. Genet. 8 (2007) 533.

[3] S.F. Mitchell, R. Parker, Mol. Cell 54 (2014) 547.

[4] S. Gerstberger, M. Hafner, T. Tuschl, Nat. Rev. Genet. 15 (2014) 829.

[5] N. H. Gehring, E. Wahle und U. Fischer, Trends Biochem Sci (2017) xxx.

[6] A.G. Baltz, M. Munschauer, B. Schwanhäusser, A. Vasile, Y. Murakawa, M. Schueler, N. Youngs, D. Penfold-Brown, K. Drew, M. Milek, E. Wyler, R. Bonneau, M. Selbach, C. Dieterich, M. Landthaler, Mol. Cell 46 (2012) 674.

[7] A. Castello, B. Fischer, K. Eichelbaum, R. Horos, B.M. Beckmann, C. Strein, N.E. Davey, D.T. Humphreys, T. Preiss, L.M. Steinmetz, J. Krijgsveld, M.W. Hentze, Cell 149 (2012) 1393.

[8] B. Beckmann, R. Horos, B. Fischer, A. Castello, K. Eichelbaum, A.-M. Alleaume, T. Schwarzl, T. Curk, S. Foehr, W. Huber, J. Krijgsveld, M. Hentze, Nature Communications 6 (2015) 10127.

[9] C. Kwon, H. Yi, K. Eichelbaum, S. Föhr, B. Fischer, K. You, A. Castello, J. Krijgsveld, M. Hentze, N. Kim, Nature Structural & Molecular Biology 20 (2013) 1122.

[10] A. Liepelt, I.S. Naarmann-de Vries, N. Simons, K. Eichelbaum, S. Föhr, S.K. Archer, A. Castello, B. Usadel, J. Krijgsveld, T. Preiss, G. Marx, M.W. Hentze, D.H. Ostareck, A. Ostareck-Lederer, Mol. Cell Proteomics 15 (2016) 2699.

[11] Y. Liao, A. Castello, B. Fischer, S. Leicht, S. Föehr, C.K. Frese, C. Ragan, S. Kurscheid, E. Pagler, H. Yang, J. Krijgsveld, M.W. Hentze, T. Preiss, Cell Rep 16 (2016) 1456.

[12] A. Matia-González, E. Laing, A. Gerber, Nature Structural & Molecular Biology 22 (2015) 1027.

[13] H.-H.H. Wessels, K. Imami, A.G. Baltz, M. Kolinski, A. Beldovskaya, M. Selbach, S. Small, U. Ohler, M. Landthaler, Genome Res. 26 (2016) 1000.

[14] V. Sysoev, B. Fischer, C. Frese, I. Gupta, J. Krijgsveld, M. Hentze, A. Castello, A. Ephrussi, Nat Commun 7 (2016) 12128.

[15] M. Reichel, Y. Liao, M. Rettel, C. Ragan, M. Evers, A.-M.M. Alleaume, R. Horos, M.W. Hentze, T. Preiss, A.A. Millar, Plant Cell 28 (2016) 2435.

[16] C. Marondedze, L. Thomas, N. Serrano, K. Lilley, C. Gehring, Sci Reports 6 (2016) 29766.

[17] E.M. Bunnik, G. Batugedara, A. Saraf, J. Prudhomme, L. Florens, K.G. Le Roch, Genome Biol. 17 (2016) 147.

[18] D. Nandan, S.A. Thomas, A. Nguyen, K.-M.M. Moon, L.J. Foster, N.E. Reiner, PLoS ONE 12 (2017) e0170068.

[19] V. Despic, M. Dejung, M. Gu, J. Krishnan, J. Zhang, L. Herzel, K. Straube, M.B. Gerstein, F. Butter, K.M. Neugebauer KM. Genome Res. (2017) doi: 10.1101/gr.215954.116.

[20] D.D. Licatalosi, A. Mele, J.J. Fak, J. Ule, M. Kayikci, S.W. Chi, T.A. Clark, A.C. Schweitzer, J.E. Blume, X. Wang, J.C. Darnell, R.B. Darnell, Nature 456 (2008) 464.

[21] M. Hafner, M. Landthaler, L. Burger, M. Khorshid, J. Hausser, P. Berninger, A. Rothballer, M. Ascano, A.-C.C. Jungkamp, M. Munschauer, A. Ulrich, G.S. Wardle, S. Dewell, M. Zavolan, T. Tuschl, Cell 141 (2010) 129.

[22] J. König, K. Zarnack, G. Rot, T. Curk, M. Kayikci, B. Zupan, D. Turner, N. Luscombe, J. Ule, Nature Structural & Molecular Biology 17 (2010) 909.

[23] E. Nostrand, G. Pratt, A. Shishkin, C. Gelboin-Burkhart, M. Fang, B. Sundararaman, S. Blue, T. Nguyen, C. Surka, K. Elkins, R. Stanton, F. Rigo, M. Guttman, G. Yeo, Nature Methods 13 (2016) 508.

[24] J.W. Hockensmith, W.L. Kubasek, W.R. Vorachek, P.H. von Hippel, J. Biol. Chem. 261 (1986) 3512.

[25] R. Brimacombe, W. Stiege, A. Kyriatsoulis, P. Maly, Meth. Enzymol. 164 (1988) 287.

[26] M. Ascano, M. Hafner, P. Cekan, S. Gerstberger, T. Tuschl, Wiley Interdiscip Rev RNA 3 (2012) 159.

[27] A.-C.C. Jungkamp, M. Stoeckius, D. Mecenas, D. Grün, G. Mastrobuoni, S. Kempa, N. Rajewsky, Mol. Cell 44 (2011) 828.

[28] G. Singh, A. Kucukural, C. Cenik, J.D. Leszyk, S.A. Shaffer, Z. Weng, M.J. Moore, Cell 151 (2012) 750.

[29] L. Dölken, Z. Ruzsics, B. Rädle, C.C. Friedel, R. Zimmer, J. Mages, R. Hoffmann, P. Dickinson, T. Forster, P. Ghazal, U.H. Koszinowski, RNA 14 (2008) 1959.

[30] A. Andrus, R.G. Kuimelis, Curr Protoc Nucleic Acid Chem Chapter 10 (2001) Unit 10.6.

[31] J. Cox, M.Y. Hein, C.A. Luber, I. Paron, N. Nagaraj, M. Mann, Mol. Cell Proteomics 13 (2014) 2513.

[32] W.F. Marzluff, Curr. Opin. Cell Biol. 17 (2005) 274.

[33] H. Chang, J. Lim, M. Ha, N. Kim, Molecular Cell 53 (2014) 1044.

[34] J.-E. Park, H. Yi, Y. Kim, H. Chang, N. Kim, Molecular Cell 62 (2016) 462.

[35] J. Lim, M. Lee, A. Son, H. Chang, N. Kim, Genes & Development 30 (2016) 1671.

[36] J.J. Quinn, H.Y. Chang, Nat. Rev. Genet. 17 (2016) 47.

[37] K. Burger, B. Mühl, M. Kellner, M. Rohrmoser, A. Gruber-Eber, L. Windhager, C. Friedel, L. Dölken, D. Eick, RNA Biology 10 (2013) 1623.

[38] J. Cox, M. Mann, Nature Biotechnology 26 (2008) 1367.

[39] J. Cox, M.Y. Hein, C.A. Luber, I. Paron, N. Nagaraj, M. Mann, Mol. Cell Proteomics 13 (2014) 2513.

[40] A.G. Jacob, C.W. Smith, Hum Genetics (2017) doi:10.1007/s00439-017-1791-x

Figure Legends

Fig. 1 – Detailed graphical representation of the mRNA interactome capture protocol for mammalian cell culture systems. Cells are crosslinked (a. cCL, b. PAR-CL, c. FA) and lysed, then cell extracts are subjected to three consecutive rounds of oligo(dT) affinity purification. After each round, poly(A)+ RNA is collected by heat elution. Eluates are subjected to nuclease treatment for RNA removal.

Fig. 2 – Quality control and analysis of oligo(dT) eluates by SDS-PAGE and silver stain. Shown from left to right are input (I), RNase control (R) and the oligo(dT) eluates from cCL, PAR-CL and FA-crosslinked samples (+) and non-crosslinked controls (-).

Fig. 1

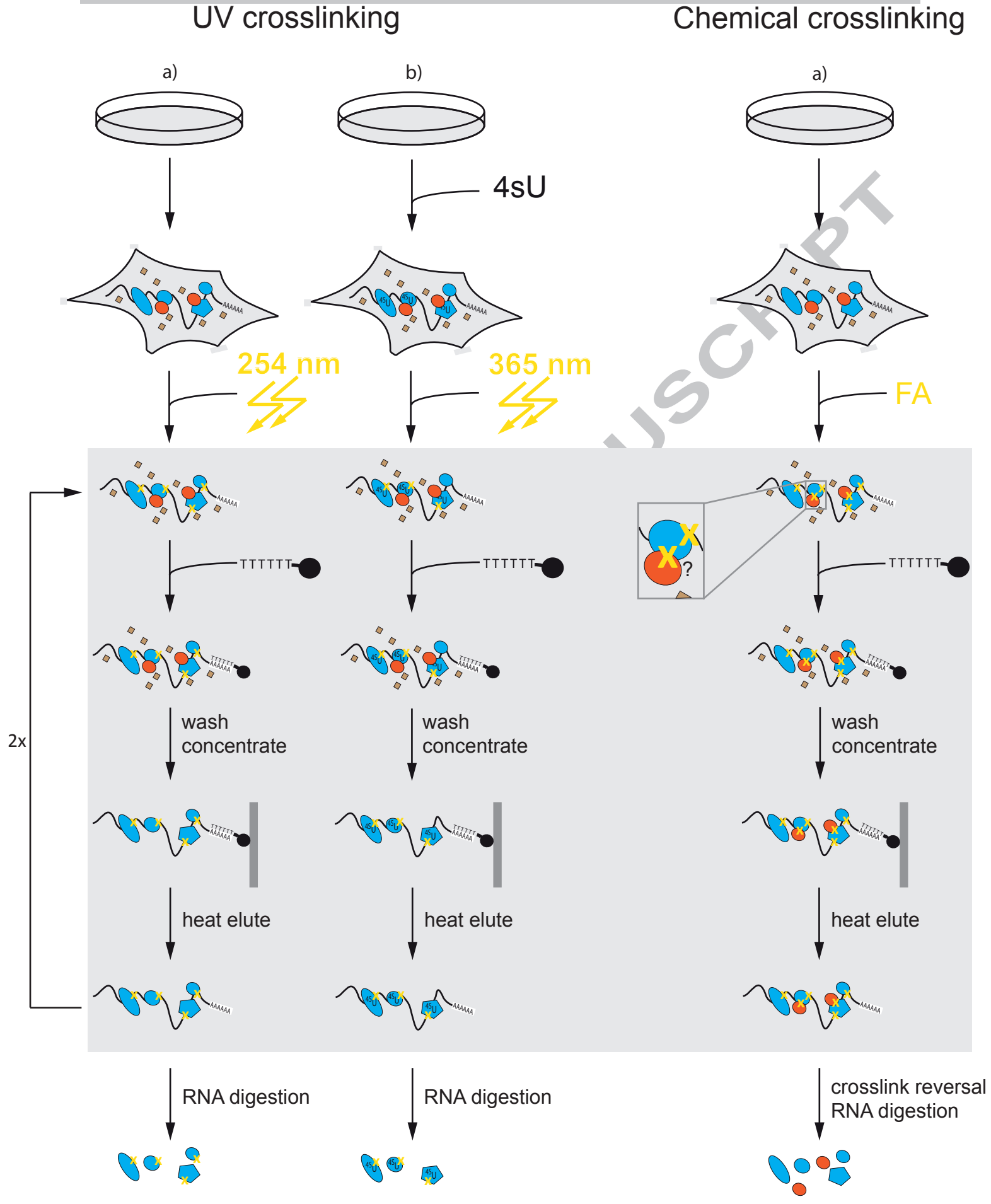

Fig. 2

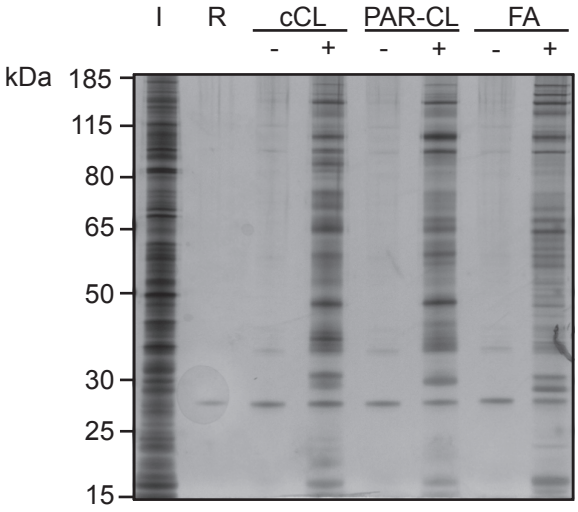

Highlights

- protein-mRNA complexes are stabilized by chemical or photocrosslinking
- isolation of crosslinked protein-RNA complexes by oligo(dT) affinity purification
- mRNA interactome capture identifies mRNA-binding proteins